

Bose-Einstein condensation from a gluon transport equation

B A Harrison and A Peshier

Department of Physics, University of Cape Town, Private Bag X3, Rondebosch 7701, South Africa

E-mail: hrrbre012@myuct.ac.za

Abstract. We present a novel numerical scheme to solve the QCD Boltzmann equation in the soft scattering approximation, for the quenched limit of QCD. Using this we can readily investigate the evolution of spatially homogeneous systems of gluons distributed isotropically in momentum space. We numerically confirm results of Blaizot et al [1, 2], in particular that for so-called “overpopulated” initial conditions, a (transient) Bose-Einstein condensate could emerge during equilibration, in a finite time. Beyond that, we analyze the dynamics of the formation of this condensate. The scheme is extended to systems with cylindrically symmetric momentum distributions, in order to investigate the effects of anisotropy. In particular, we compare the rates at which isotropization and equilibration occur. We also compare our results from the soft scattering scheme to the relaxation time approximation.

1. Introduction

The study of quark-gluon plasma (QGP), the phase of strongly interacting matter formed as a result of relativistic nuclear collisions and consisting of quasi-free quarks and gluons, is of increasing relevance in modern physics [3]. It represents a testing ground for the Standard Model, as well as for finite temperature field theory and possible grand unification theories. It is also of cosmological significance, as the early universe was dominated by this phase of matter.

Experiments at the Relativistic Heavy Ion Collider (RHIC) and Large Hadron Collider (LHC) allow us to probe the energy scales at which the QGP is produced. Inferring its properties and phenomenological behaviour is a central goal of the heavy ion programs at these facilities. The theoretical tools that have been developed to describe it are manifold, as the various stages of a heavy ion collision represent very different physical regimes that demand similarly diverse mathematical formalisms to describe (see Fig. 1).

Prior to the collision, the nuclei are accelerated to near-light speed, with a Lorentz factor on the order of 100. They are therefore subject to strong Lorentz contraction along the beam axis. At these energies, the lifetime of gluons emitted from the valence quarks or other gluons is long enough to allow additional emissions of soft gluons from themselves. This process keeps increasing the number density of gluons until saturation occurs as recombination of gluons becomes non-negligible, forming the state of matter called the Color Glass Condensate (CGC). This regime of large gluon number is well approximated by classical dynamics [4-6].

In the following stage, a large number of gluons are liberated from the CGC. These gluons form a dense, off-equilibrium state called the glasma. Extensive hydrodynamic analyses of HIC indicate that as the medium expands, rapid thermalization occurs (characteristic time on

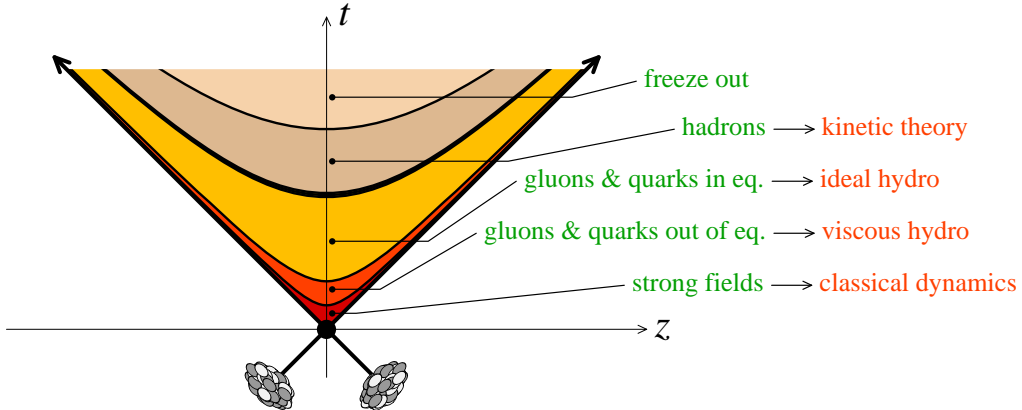


Figure 1. The stages of a heavy ion collision (from [3]).

the order of 1 fm) and a QGP in local equilibrium forms. The speed of this thermalization is indicative of strong interactions. As the medium continues to expand and decrease in temperature, it eventually drops below the deconfinement temperature ($T_c \approx 170$ MeV) and hadronization occurs [7-10].

Using relativistic kinetic theory as an alternative, in some respects more fundamental, approach to viscous hydrodynamics, we aim to describe the collective behaviour of the QGP from the earliest pre-equilibrium stages through thermalization and eventual freeze-out. To this end we numerically solve the relativistic Boltzmann equation.

2. The Boltzmann Transport Equation

The fundamental equation of kinetic theory is the Boltzmann transport equation. It is a non-linear integro-differential equation, for our purposes governing the evolution of the distribution function of a dilute gas of gluons “in a box”. (Quarks are omitted as the relevant regime is gluon-dominated). For a spatially homogeneous system under the assumption that $2 \rightarrow 2$ processes dominate, it can be written as

$$\partial_t f = \frac{1}{2} \int \frac{d^3 p_2}{(2\pi)^3 2E_2} \frac{d^3 p_3}{(2\pi)^3 2E_3} \frac{d^3 p_4}{(2\pi)^3 2E_4} \frac{|\mathcal{M}_{12 \rightarrow 34}|^2}{2E_1} (2\pi)^4 \delta(p_1 + p_2 - p_3 - p_4) (f_3 f_4 \bar{f}_1 \bar{f}_2 - f_1 f_2 \bar{f}_3 \bar{f}_4). \quad (1)$$

Here f_i is the distribution function of particle i with 4-momentum $p_i = (E_i, p_i)$. As shorthand, we write $\bar{f}_i \equiv 1 + f_i$. The transition amplitude \mathcal{M} of binary gluon scattering reads at tree level

$$|\mathcal{M}_{12 \rightarrow 34}|^2 = 72g^4 \left[3 - \frac{tu}{s^2} - \frac{su}{t^2} - \frac{st}{u^2} \right], \quad (2)$$

where s , t and u are the familiar Mandelstam variables and g is related to the QCD coupling constant α by $g^2 = 4\pi\alpha$.

For small scattering angles, $|t| \ll s$ and expression (2) simplifies to

$$|\mathcal{M}_{12 \rightarrow 34}|^2 \approx 144g^4 \frac{s^2}{t^2}, \quad (3)$$

which is to be regulated, e.g. by making the substitution

$$\frac{1}{t^2} \rightarrow \frac{1}{(t - \mu^2)^2}, \quad (4)$$

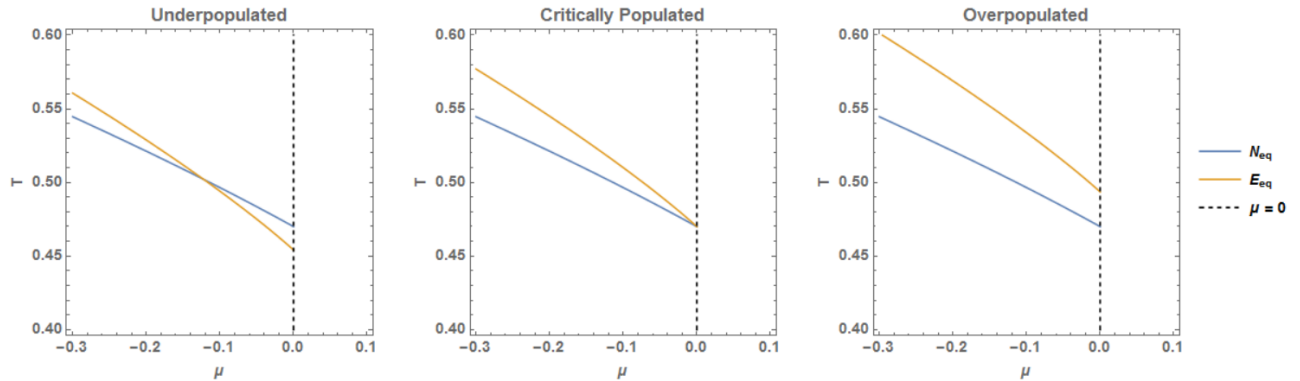


Figure 2. Contours of constant particle number and energy density at equilibrium. In the under- and critically populated cases, the values of the equilibrium parameters T and μ are found where the lines intersect. In the critically populated case, the intersection occurs at the maximum possible value of $\mu = 0$. In the overpopulated case, no real solution for $\mu < 0$ exists and a condensate is necessary to contain the excess particles.

where μ is the screening mass. While this equation is a challenge to solve, the Boltzmann H-Theorem guarantees that regardless of initial condition, the equilibrium distribution function will be a Jüttner distribution [11],

$$f_{eq}(x, p) = \left[e^{\frac{p^\alpha u_\alpha(x) - \mu(x)}{T(x)}} - 1 \right]^{-1}. \quad (5)$$

Here T , u and μ parameterize the temperature, collective flow velocity and chemical potential, respectively.

There is one caveat; there exists a class of “overpopulated” initial distribution functions (see Fig. 2) which contain more gluons than can be “accommodated” in a Jüttner distribution while maintaining particle number and energy conservation. It has been argued [1] that under the assumption of gluon number conservation, a transient equilibrium state may form with a Bose-Einstein condensate.

3. The Fokker-Planck and Relaxation Time approximations

Under the assumption that small-scattering angles dominate, it is possible to write the RHS of Eq. 1 as the divergence of a current in momentum space [1],

$$D_t f = -\nabla \cdot \mathcal{J}(p), \quad (6)$$

where \mathcal{J} reads

$$\mathcal{J}_i(p) = \frac{9}{4\pi} g^4 \mathcal{L} \int_k \mathcal{V}_{ij}(p, k) \left\{ f_p \bar{f}_p \nabla_k^j f_k - f_k \bar{f}_k \nabla_p^j f_p \right\}. \quad (7)$$

Introduced here is

$$\mathcal{V}^{ij} = (1 - v \cdot w) \delta^{ij} + (v^i w^j + v^j w^i), \quad (8)$$

where to lighten notation we have defined $p \equiv p_1$, $k \equiv p_2$ and denoted the corresponding unit vectors by $w \equiv p/p$ and $v \equiv k/k$.

In Eq. 7, \mathcal{L} is the so-called Coulomb logarithm emerging in screened interactions with vector boson exchange, $\mathcal{L} = \int_{q_{min}}^{q_{max}} \frac{dq}{q} = \ln \frac{q_{max}}{q_{min}}$ where q_{max} and q_{min} are cutoffs of the order of the

equilibrium temperature T and Debye screening mass m_D , respectively [1]. We take \mathcal{L} to be a constant of order 1 in our analysis.

It is convenient to rescale the time variable in Eq. 6 as $\tau = \frac{9}{4\pi} g^4 \mathcal{L} t$ to eliminate the constant factor in Eq. 7. The integral in currentIntegral can then be performed and yields [12]

$$\mathcal{J}(p) = I_a \nabla f + I_b f \bar{f} \hat{p} + (\nabla f \cdot \hat{p}) \mathcal{I} + (\nabla f \times \hat{p}) \times \mathcal{I}, \quad (9)$$

where $I_a = \int f \bar{f}$, $I_b = \int \frac{2f}{p}$ and $\mathcal{I} \equiv (\mathcal{I}_x, \mathcal{I}_y, \mathcal{I}_z) = \int \frac{\vec{p}}{p} f \bar{f}$ are functionals of the distribution function f .

We have constructed an efficient flux-conservative numerical scheme [12] that allows us to solve the Boltzmann equation in the Fokker-Planck approximation, (6) + (9), for initial conditions cylindrically symmetric in momentum space.

It is worth comparing this scheme to the well-known Relaxation Time Approximation (RTA),

$$\partial_t f = \frac{p^\mu u_\mu}{p_0} \frac{f_\infty - f}{\tau_r}. \quad (10)$$

where the constant τ_r is the characteristic relaxation time for which the approximation is named.

The RTA is easily solvable (and converges to the same equilibrium distribution); however it lacks QCD-specific features and as we will see yields qualitatively different behavior to the Fokker-Planck approximation, which we argue is more physically motivated.

4. Results

Figs. 3-6 show the evolution in the special case of spherically symmetric, CGC-inspired initial conditions of the form

$$f(p) = f_0 \frac{1}{e^{(p-Q)/C} + 1}, \quad (11)$$

where f_0 and C are constants and Q sets the momentum scale. For these figures, we have chosen $f_0 = 0.225$ and $C = 0.05Q$ (and $Q \rightarrow 1$), which is a moderately overpopulated initial condition where some 8% of the particles asymptotically condense. We denote the number density of the condensate by n_c .

Of particular note is the qualitative difference between the results from the Fokker-Planck and Relaxation Time Approximations. In particular, the condensate begins to form immediately in the Fokker-Planck scheme, whereas the Relaxation Time Approximation exhibits a characteristic ‘‘lag’’.

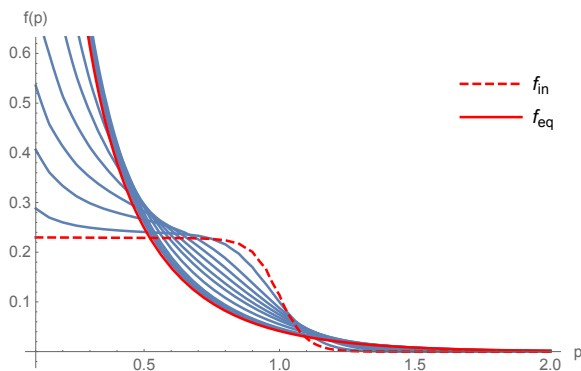


Figure 3. Evolution of an overpopulated initial condition using the Fokker-Planck approximation.

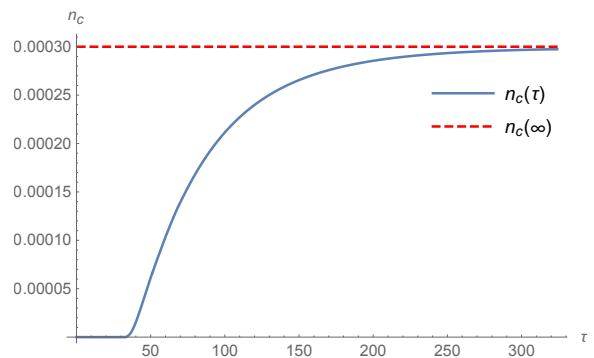


Figure 4. Corresponding evolution of the condensate for the system in Fig. 3.

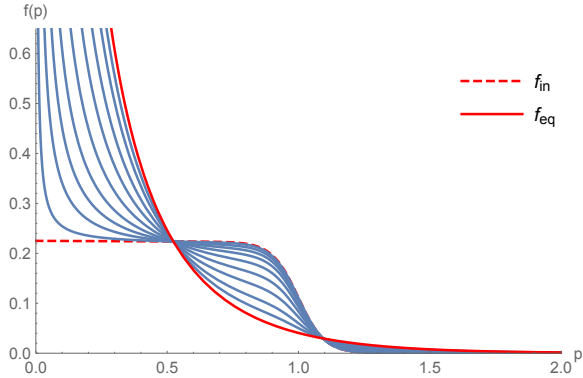


Figure 5. Evolution of an overpopulated initial condition using the Relaxation Time Approximation.

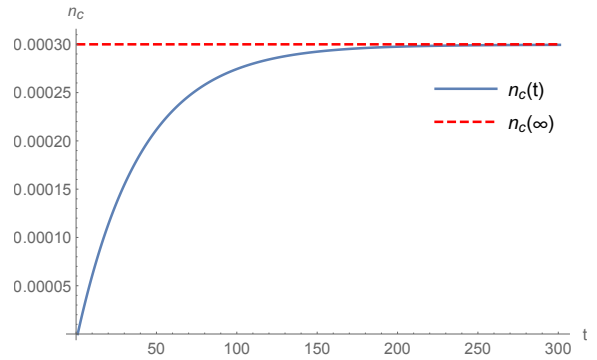


Figure 6. Corresponding evolution of the condensate for the system in Fig. 5.

Generalizing from spherically symmetric to cylindrically symmetric initial conditions, it becomes possible to explore the effects on anisotropy on the evolution of the distribution function. It is important to differentiate between isotropic distribution functions just boosted out of their rest frame and distribution functions that are “generically” anisotropic, i.e. even in their rest frame.

In order to study anisotropy of the second kind, we follow Strickland [13] and consider initial conditions of the form

$$f(\omega, p_z) \rightarrow (\sqrt{1 + \xi}) f\left(\sqrt{\omega^2 + \xi p_z^2}, p_z\right), \quad (12)$$

where $\xi > -1$ specifies the anisotropy and the factor of $\sqrt{1 + \xi}$ is a normalization to preserve particle number and energy density while varying ξ .

We can generalize our spherically symmetric initial condition (Eq. 11) using this anisotropization. Additionally (as we will see in Eq. 13) we introduce a boost parameter b which introduces a net flow in the z -direction. This can be interpreted as a boost out of the rest frame.

We are therefore interested in the family of initial conditions

$$f(\omega, p_z) = (\sqrt{1 + \xi}) \frac{f_0}{e^{\frac{1}{T}(\sqrt{\omega^2 + \xi p_z^2} + b p_z - Q)} + 1}, \quad (13)$$

where $\omega = |p|$. We extract the equilibration time by studying the entropy, evaluated towards final equilibrium. In particular we would like to compare it to the time taken for the initially anisotropic distribution function to isotropize.

To this end, as a measure of the anisotropy of a distribution function, we define the “anisotropy parameter”

$$\alpha = \frac{T_{LRF}^{22}}{T_{LRF}^{33}}, \quad (14)$$

where $T_{LRF}^{\mu\nu}$ is the energy-momentum tensor in the local rest frame. In the rest frame, for a cylindrically symmetric distribution function with some anisotropy, $T^{11} = T^{22} = P_{\perp}$ is the transverse pressure of the fluid, while $T^{33} = P_z$ is the longitudinal pressure. For an isotropic distribution they are equal; thus the ratio α must approach 1 as the system isotropizes. Analogously, the ratio of the system’s entropy S to its equilibrium entropy S_{∞} approaches 1 as the system equilibrates.

In Fig. 7, as a proof of concept we plot the evolution of the normalized entropy and anisotropy parameters associated with a representative initial condition. Fig. 8 shows a linearization of this evolution.

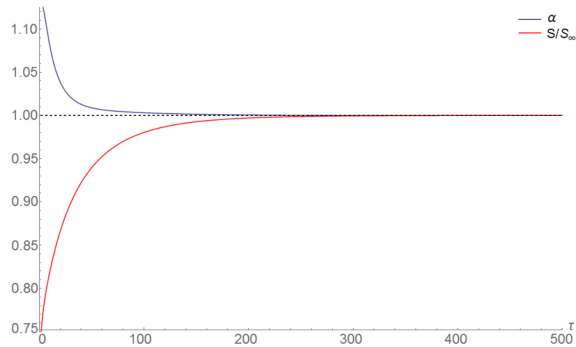


Figure 7. Evolution of the normalized entropy and anisotropy parameters.

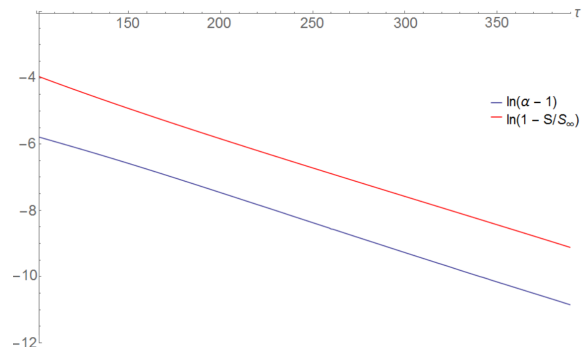


Figure 8. Linearized evolution of the normalized entropy and anisotropy parameters.

The gradients of the lines of best fit associated with the plots in Fig. 8 are identical within uncertainty (obtainable e.g. using statistical resampling methods) which corroborates that the rates of isotropization and equilibration are strongly correlated.

5. Conclusion

In summary, we have developed a numerical scheme to solve the relativistic Boltzmann equation for gluons in the small-scattering approximation under the assumption of cylindrically symmetric initial conditions and spatial homogeneity. Among our results, we have presented an argument for the formation of a transient Bose-Einstein condensate state for certain initial conditions. We have investigated the rate at which an anisotropic distribution function becomes isotropic and compared it to the rate of thermalization. Further, we have compared these results to the relaxation-time approximation to the Boltzmann equation.

Scope for further extension of this scheme exists, and such an extension is planned. In particular, it is desirable to extend the scheme to remove the assumption of spatial homogeneity and describe systems without symmetry assumptions in which the above scheme would essentially represent a single spatial cell. A challenge is the fact that the computational complexity scales geometrically with each additional degree of freedom - the so-called “curse of dimensionality”. (Boltzmann equation solvers as well as hydro-codes typically rely on assumptions of symmetry, and for good reason).

References

- [1] Blaizot J-P, Liao J and McLerran L 2013 *Nuclear Physics A* **920** 58
- [2] Blaizot J-P, Liao J and Mehtar-Tani Y 2017 *Nuclear Physics A* **961** 37
- [3] Gelis F 2012 *Journal of Physics: Conference Series* **381** 12021
- [4] McLerran L and Venugogalan R *Physical Review D* 1994 **49** 2233
- [5] Gelis F 2016 *Quark-Gluon Plasma* 5 67
- [6] Weigert H 2005 *Progress in Particle and Nuclear Physics* **55** 461
- [7] Heinz U W and Kolb P F 2002 *Nuclear Physics A* **702** 269
- [8] Romatschke P and Romatschke U 2007 *Physical Review Letters* **99** 172301
- [9] Ollitrault J-Y 2008 *European Journal of Physics* **29** 275
- [10] Romatschke P and Romatschke U 2017 arXiv:1712.05812[nucl-th]
- [11] Rezzolla L and Zanotti O 2013 *Relativistic Hydrodynamics* (Oxford: OUP)
- [12] Harrison B and Peshier A 2019 *Particles* **2** 231
- [13] Schenke B and Strickland M 2006 *Physical Review D* **74** 65004